Near-Field Magnetic Induction MIMO Communication Using Heterogeneous Multi-pole Loop Antenna Array for...

Article *in* IEEE Transactions on Antennas and Propagation · May 2016

DOI: 10.1109/TAP.2016.2539371

6 authors, including:

Han-Joon Kim
Daegu Gyeongbuk Institute of Science and T…

Kyoung-Sub Oh

Jihwan Choi
Daegu Gyeongbuk Institute of Science and T…

Ji-Woong Choi
Daegu Gyeongbuk Institute of Science and T…

Near-Field Magnetic Induction MIMO Communication Using Heterogeneous Multipole Loop Antenna Array for Higher Data Rate Transmission

Han-Joon Kim, *Student Member, IEEE*, Jinho Park, *Member, IEEE*, Kyoung-Sub Oh, Jihwan P. Choi, *Member, IEEE*, Jae Eun Jang, and Ji-Woong Choi, *Senior Member, IEEE*

***Abstract*—In this paper, we propose a novel method realizing multi-input–multi-output (MIMO) transmission in near-field magnetic induction (NFMI) communication for increasing channel capacity where limited capacity is a major bottleneck problem in magnetic communication systems. Since conventional magnetic communication systems using the same antenna patterns cannot easily implement MIMO transmission due to strong crosstalk between transmitters, we propose heterogeneous antenna arrays with multipole antennas, enabling crosstalk cancellation. We confirm the crosstalk cancellation of the proposed antenna array through numerical simulations and experiments, and verify the capacity enhancement of the proposed NFMI communication system over conventional NFMI communication schemes.**

***Index Terms*—Antenna array, crosstalk cancellation, electromagnetic coupling, electromagnetic induction, magnetic communication, magnetic field, multi-input–multi-output (MIMO), near-field communication (NFC).**

I. Introduction

In RECENT years, there has been strong demand for communication systems operating in special channel environments that have a high permittivity, such as underground [1], underwater [2], armory [3], and biological tissues [4]. Conventional radio frequency (RF) communications, which are based on electromagnetic (EM) wave propagation, cannot provide reliable communication under these high permittivity channels *due to significant EM loss*, resulting in large path loss. In contrast, a near-field magnetic induction (NFMI) communication system can enhance communication quality at the near-field in high permittivity channel environments since the magnetic permeability, which mainly determines the path loss of magnetic waves, of high permittivity materials is generally similar to the air, enabling moderate path loss comparable to that in the air [5]. Therefore, NFMI communication systems are more beneficial than EM communication systems in these channels. However, applications of NFMI communication systems are limited due to limited channel capacity, high sensitivity to alignment error, and short communication range [6]. The communication range depends on the near-field range in relation to frequency. For example, when carrier frequency f_c is 13.56 MHz, the near-field range $\lambda/2\pi$ is equal to 3.5 m, which is far enough for MI communication applications, such as wireless body area networking and indoor wireless power transfer (WPT).

In this paper, we focus on the limited channel capacity problem. The data rate of near-field communication (NFC) is 106–848 kbps [7], where conventional NFC applications do not require high data rate transmission in general. However, in the near future, higher data rate NFC systems are expected to be required for diverse applications such as multimedia data transmission, high-resolution personal information and security code transfer, medical applications, and wireless localization. For example, e-passport has additional personal information and complex security codes such as fingerprints and pictures to be shared. Smart posters enable payment and ticket reservation functions using mobile devices. Furthermore, medical applications such as artificial retina, cochlear implants, and capsule endoscopes may require high-resolution data transfer to obtain high-quality signal. Table I shows the data rate requirements of existing medical applications [8], where we can easily find high data rate applications over 1 Mbps. To satisfy these high data applications, magnetic communications need to increase the channel capacity.

Recent studies of magnetic communication techniques have great potential to solve the limited capacity problem and to enhance conventional magnetic communication systems in various high permittivity channel environments. Defining WPT efficiency as the ratio of received power to total *EM loss*, Poon

Manuscript received February 05, 2015; revised October 02, 2015; accepted February 20, 2016. Date of publication March 08, 2016; date of current version May 03, 2016. This work was supported in part by the Basic Science Research Program through the National Research Foundation of Korea (NRF) funded by the Ministry of Science, ICT and Future Planning (NRF-2015R1A2A2A01008218), in part by the DGIST R&D Program of the Ministry of Science, ICT and Future Planning (16-BD-0404), and in part by the Robot Industry Fusion Core Technology Development Project of the Ministry of Trade, Industry and Energy of KOREA (10052980).

H.-J. Kim, J. P. Choi, J. E. Jang, and J.-W. Choi are with the Department of Information and Communication Engineering, Daegu Gyeongbuk Institute of Science and Technology (DGIST), Daegu 771-873, South Korea (e-mail: hanjoonkim@dgist.ac.kr; jhchoi@dgist.ac.kr; jang1@dgist.ac.kr; jwchoi@dgist.ac.kr).

J. Park is with TeraSquare Co. Ltd, Seoul 135-920, South Korea (e-mail: jpark@terasquare.co.kr).

K.-S. Oh is with Gamma Nu, Inc., Hwasung 445-811, South Korea (e-mail: ksfaraday@msn.com).

Color versions of one or more of the figures in this paper are available online at http://ieeexplore.ieee.org.

Digital Object Identifier 10.1109/TAP.2016.2539371

TABLE I
DATA RATE REQUIREMENT IN MEDICAL APPLICATIONS

Application	Target data-rate
Deep brain stimulation	1 Mbps
Hearing aid	200 kbps
Capsule endoscope	1 Mbps
Drug dosage	< 1 kbps
ECG	72 kbps (500 Hz sample, 12-bit ADC, 12 channels)
EEG	86.4 kbps (300 Hz sample, 12-bit ADC, 24 channels)
EMG	1.536 Mbps (8 kHz sample, 16-bit ADC, 12 channels)
O2/CO2/BP/respiration/glucose monitoring, accelerometer	< 10 kbps
Audio	1 Mbps
Video/medical imaging	< 10 Mbps

proved that high frequency is optimal for implantable small-loop antennas in biological tissues, e.g., GHz and sub-GHz for mm- and cm-level antennas, respectively [9]. This high frequency may easily enhance the channel capacity by allocating larger bandwidth which is more plausible at the high-frequency band. However, this solution may not be applicable in general since the optimality at GHz frequency is valid in the limited cases where antenna size is given to be small and the antenna is surrounded by biological material.

Sun and Akyildiz have studied to increase the communication range and channel capacity of underground magnetic communication systems using the MI waveguide proposed by Shamonina *et al.* [10]. Sun and Akyildiz applied an MI waveguide to wireless communication applications and developed a spread resonance (SR) strategy in which each coil in the MI waveguide uses the same resonant frequency, to improve the communication range and capacity [6]. In the case of the SR strategy MI waveguide, each coil has a unique and optimal resonance frequency which can lead to considerable improvement of channel capacity. However, the SR strategy requires significant system complexity because each relay coil has to be designed to have a different resonant frequency.

Furthermore, Masihpour and Agbinya proposed new MI waveguide relaying models, called master assistant magnetic induction, to extend the range and increase the data rate of medical implants and underground communications [11]. In their proposed models, each transmitted signal reaches a receiver through different paths from different relay nodes which transmit the same data. Consequently, this effect enhances the signal which can propagate longer and provides a higher data rate within the channel. The data rate can be further increased using the optimal quality factor. This proposed method may be appropriate in sensor-networks that include many relay nodes. However, because there are extra nodes for relaying, it is not suitable for peer-to-peer communication. Furthermore, their study assumed an ideal situation which does not consider misalignment among relay nodes and the receiver. When misalignment is considered, channel capacity would be reduced significantly. In addition, this group tried to analyze the channel capacity of near-field magnetic multi-input–multi-output (MIMO) [12]. However, they did not consider the crosstalk of signals from multiple transmitters, where the crosstalk is interference caused by undesired inductive coupling among antennas, which cannot be avoided with conventional antenna arrays.

Gottula and Warnick showed possibility of 3×3 NFMI MIMO array structure which is composed of three orthogonally arranged hollow-core ferrite-loaded loop antennas to obtain high data rate [13]. Since their perpendicularly arranged antenna array can provide partially isolated multiple streams while complete isolation is not guaranteed, it can support higher data rate using the partial crosstalk cancellation and also employing different resonant frequencies for each antenna at the cost of bandwidth increase. This structure can support up to three streams according to the number of axis in free space, i.e., x, y, and z axis.

To obtain enhanced channel capacity, MIMO technology can be one of promising solutions. This paper proposes NFMI MIMO system without crosstalk using heterogeneous multipole loop antenna array which allows crosstalk cancellation. The main contributions are highlighted into the following three aspects.

1) All kinds of crosstalk due to magnetic coupling can be *significantly reduced*: Conventional magnetic MIMO systems cannot easily remove the crosstalk which is caused by magnetic coupling. The proposed heterogeneous antenna array structure can remove all kinds of crosstalk among array components, unlike prior studies [12], [13].
2) More than three multiple parallel streams can be supported: In previous study [13], they cannot support more than three streams. The proposed NFMI MIMO can obtain multiple parallel streams as many as the number of array components.
3) Channel capacity enhancement is available without complicated signal processing: The conventional RF MIMO can achieve parallel spatial multichannels using complicated signal processing such as singular value decomposition (SVD) and channel estimation. The proposed scheme can realize parallel multichannels without complicated signal processing by crosstalk cancellation. The proposed magnetic MIMO structure enables not only channel capacity enhancement but also simultaneous information and power transmission which is helpful for various mobile and medical devices. We also confirm that it is relatively robust to the misalignment error.

This paper is organized as follows. In Section II, we propose a heterogeneous multipole antenna pattern that enables crosstalk reduction, which is verified by numerical simulations and experiments. Section III presents the channel characteristic and capacity of the NFMI MIMO communication system employing the proposed antenna pattern. Section IV discusses practical issues, such as misalignment. Finally, conclusion is drawn followed by suggestions on potential applications in Section V.

II. Crosstalk Cancellation Using Heterogeneous Multipole Antenna Array

A. *Concept of Crosstalk Cancellation*

MIMO is a typical method used in EM communications to increase capacity without additional power or bandwidth through independent message transmission from multiple antennas in parallel. Signals from transmit antennas usually arrive at each receive antenna; each receive antenna receives signals from all the transmit antennas, resulting in spatial interference. This spatial interference can be compensated at the receiver using linear or nonlinear equalizers, or it can be transformed into parallel channels without spatial interference using SVD [14]. However, there is little interference among the transmit antennas in EM communications. On the other hand, in MI communications utilizing magnetic inductive coupling, coupling between transmit antennas creates crosstalk among the transmit signals, which induces iterative coupling back and forth between the signals from different transmit antennas. For example, Fig. 1 presents the pattern of an NFMI MIMO antenna array comprising circular loop antennas, where the desired transfer coefficients S21 and S43 are smaller than crosstalk S31 between transmit antennas and crosstalk S42 between receive antennas, where SYX denotes a signal from antenna X to antenna Y. While the interference signals S41 and S23 may be compensated through signal processing, the crosstalk S42 and S31 from the lateral coils need to be small enough not to cause severe crosstalk through successive coupling. Therefore, to enhance capacity through multiple stream transmission in parallel, NFMI communication systems have to reduce the crosstalk. We propose an NFMI MIMO scheme which has a crosstalk cancellation effect using a heterogeneous multipole loop antenna array as seen in Fig. 2. Crosstalk cancellation enables by the "fully decoupling" state in which there is no coupling between *transmit and receive antennas*. Mutual inductance M_{ij} is the quantitative description of the coupling between two conductor loops i and j, and coupling coefficient k can give a qualitative prediction [15]. These two important factors are given by

$$M_{12} = \frac{\mu_0 H_1 N_2 A_2}{I_1} \tag{1}$$

and

$$k = \frac{M_{12}}{\sqrt{L_1 L_2}} \tag{2}$$

where μ_0 is the permeability of vacuum; H_i is the normal direction magnetic field strength to the loop, which is caused by current I_i; I_i is the current on loop i; N_i is the number of turns in loop i; A_i is the area of loop i; and L_i is the inductance of loop i. When the coupling coefficient is 0, two conductors are in the fully decoupling state, while two conductors are in the total coupling state if the coupling coefficient is 1. To make the fully decoupling state, we need to nullify the magnetic field sum from other conductors according to the definition of the coupling coefficient. Usually, the fully decoupling state is made available by *large separation* or magnetic shielding between the antennas. Since these conditions cannot be easily met in practical communication scenarios, in this study, we created the fully decoupling state by using multipole loop antennas. Circular loop antennas have two magnetic poles and generate a magnetic field in one direction. On the other hand, multipole loop antennas can generate multiple magnetic poles and thus have magnetic fields in several directions.

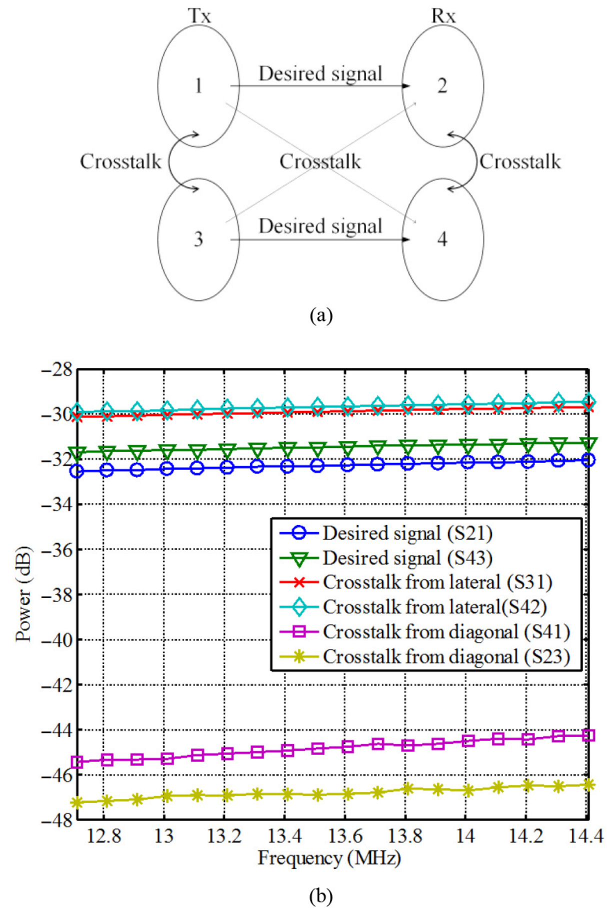

Fig. 1. (a) MIMO structure using conventional circular loop antenna array. (b) Experimental result of conventional circular loop antenna array MIMO.

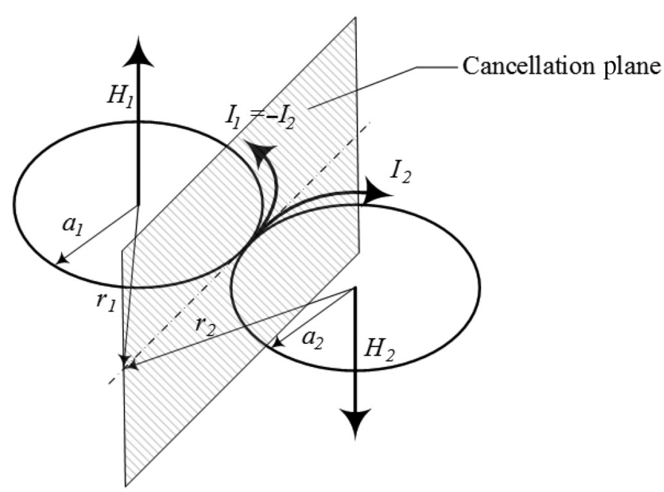

Fig. 2. Quadrupole loop antenna and its cancellation plane.

When multipole loop antennas satisfy a specific condition, these multiple magnetic fields can cancel each other.

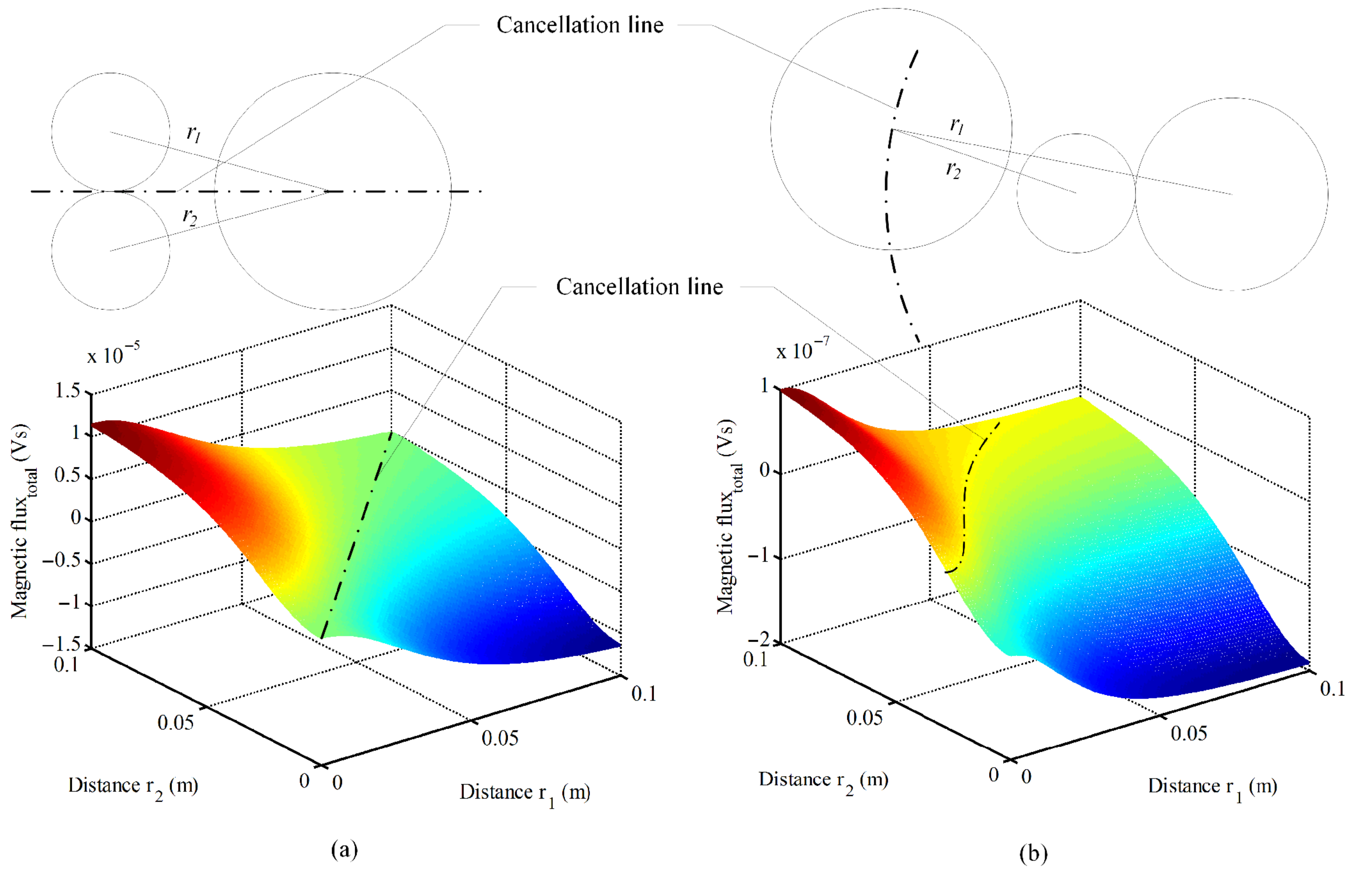

Fig. 3. (a) Cancellation plane of balanced quadrupole loop antenna. (b) Cancellation plane of unbalanced quadrupole loop antenna.

We remove the crosstalk through this cancellation effect. A quadrupole loop antenna, which looks like the number "8" as shown in Fig. 2, has the typical structure of multipole loop antennas. Usually, this type of coil is used in transcranial magnetic stimulation [16], traffic detection [17], and dual polarization antennas [18]. To make an opposite direction current in each loop of the quadrupole loop antenna, an antenna port is placed in the middle of the quadrupole loop antenna. Each current can make an opposite direction magnetic field in each loop of the quadrupole loop antenna, i.e., $I_1 = -I_2$ as seen in Fig. 2. Opposite magnetic fields cancel each other at the same distance from the center of each loop when these loops have the same radius and number of turns. We can prove the cancellation in a two-dimensional (2-D) plane using the H field. Similarly, it can be easily extended to a three-dimensional (3-D) plane. A magnetic field is denoted by

$$H = \frac{INa^2}{2\sqrt{(a^2+r^2)^3}} \tag{3}$$

in quasi-static analysis, where a is the loop radius, r is the distance from the center of a loop, and both opposite magnetic fields $\boldsymbol{H}_1$ and $\boldsymbol{H}_2$ can make a total magnetic field $\boldsymbol{H}_{total}$, which is given by

$$H_{total} = H_1 + H_2 = \frac{I_1 N_1 a_1^2}{2\sqrt{(a_1^2+r_1^2)^3}} + \frac{I_2 N_2 a_2^2}{2\sqrt{(a_2^2+r_2^2)^3}}. \tag{4}$$

When H_1 and H_2 have equal amplitudes in opposite directions, the total magnetic field H_{total} is equal to 0, enabling the fully decoupling state, i.e., crosstalk cancellation. Here, the total magnetic field can be manipulated by changing several parameters of the loop antenna, such as radius a_i of loop i, the number of turns N_i in loop i, and the distance r_i from the center of loop i. Therefore, these parameters can be set to create cancellation conditions at a specific point. We can define the cancellation plane or a region which comprises these cancellation points as seen in Fig. 2. Two magnetic loops can create cancellation conditions depending on geometric parameters of the antenna, such as shape, radius, the number of loops in a multipole loop antenna, and distance. When each center of antenna *A* is located on the cancellation plane of another antenna *B*, there is no crosstalk from antenna *B* to antenna *A*. Using this principle, we can make transmit or receive antennas experience no crosstalk by locating antennas on the cancellation planes of other transmit antennas. For crosstalk cancellation with the heterogeneous multipole loop antenna array, the following condition needs to be satisfied:

$$\frac{N_1 a_1^2}{\sqrt{(a_1^2+r_1^2)^3}} = \frac{N_2 a_2^2}{\sqrt{(a_2^2+r_2^2)^3}}. \tag{5}$$

When all parameters are fixed except r_2 in Fig. 3, we can derive the cancellation distance from the center of loop as

$$r_2 = \left(\sqrt[3]{\frac{N_2^2 a_2^4 (a_1^2+r_1^2)^3}{N_1^2 a_1^4}} - a_2^2\right)^{\frac{1}{2}}. \tag{6}$$

Fig. 3(a) presents the cancellation plane of the basic heterogeneous cancellation array, which comprises a circular loop and a balanced quadrupole loop antenna on a 2-D plane. Note that, when each of quadrupole loop antenna has the same radius as in Fig. 3(a), the cancellation plane which is a straight plane does not vary according to the radius of the loop where the points in the plane are located at the same distance from each center of the loop. Unlike Fig. 3(a), Fig. 3(b) shows a curved cancellation plane at the smaller loop side produced by an unbalanced quadrupole loop antenna with different size loops. The curvature of this cancellation plane increases as the relative difference of the two loop radius increases. Thus, we can realize parallel MIMO transmission using the proposed antenna array such that there is no crosstalk or interference among the antennas except the desired transmit and receive antenna pairs, i.e., $S41 = S23 = S31 = S42 = 0$ in Fig. 1. This is quite similar to parallel spatial multiplexing MIMO using SVD in EM communication, where interference cancellation is not required at the receiver, facilitating MIMO receiver implementation in the NFMI system.

B. Verification of Crosstalk Cancellation Via Simulation

In this section, we prove the crosstalk cancellation using high-frequency structure simulation (HFSS) [19]. Fig. 4 shows simulation models which are a conventional circular loop antenna array MIMO and the heterogeneous multipole loop antenna array MIMO. All the antennas are designed to be printed antennas for reliable comparison with experimental results. The specific parameters were set as follows: radius a_1 of the circular loop antenna is 100 mm; radius a_2 of the loops in the balanced quadrupole loop antenna is 95 mm; the patch width w is 10 mm; the copper thickness t is 88 μm; distance d between arrays is 220 mm; and distance h between the transmitter array and receiver array is 200 mm. The antenna material is copper, and the substrate is FR4. It is assumed to have no environmental or background noise to focus on the crosstalk signal. Except the desired signals S21 and S43, other signals are considered crosstalk, e.g., S31, S41, S23, and S42.

The gain of each signal is plotted in Fig. 5. In the case of the conventional circular loop antenna array shown in Fig. 4(a), the desired signal is stronger than crosstalk signals by about 6 dB without noise, implying that the signal-to-interference-and-noise power ratio (SINR) i.e., $(\mathrm{S43}/(\mathrm{S41}+\mathrm{S42}))(\mathrm{dB})$ or $(\mathrm{S21}/(\mathrm{S23}+\mathrm{S42}))(\mathrm{dB})$ is no more than 6 dB. Furthermore, the SINR decreases if the noise is included, as seen in the next section where experimental results are presented. When the heterogeneous multipole antenna array is applied to an NFMI MIMO communication system, as in Fig. 4(b), we can verify the huge reduction of crosstalk. As seen in Fig. 5(b), an SINR of about 40 dB is achieved, which is $10^{3.4}$ times that of the conventional circular loop antenna array. In this case, desired signals are isolated from each other by the crosstalk cancellation effect of the quadrupole loop antenna, enabling parallel MIMO transmission. Note also that the quadrupole loop antenna has smaller gain than the circular loop antenna, e.g., around 9 dB in Fig. 5(b) with similar radius of 100 and 95 mm for the circular and quadrupole antennas, respectively, due to a self-cancellation effect. This loss rapidly increases as the radius of the quadrupole antenna decreases. Thus, to obtain equivalent power, based on the numerical simulation results, about 30% longer radius is required for the quadrupole antenna compared to the circular antenna, implying that larger size antenna is recommended to achieve similar gain for the parallel streams.

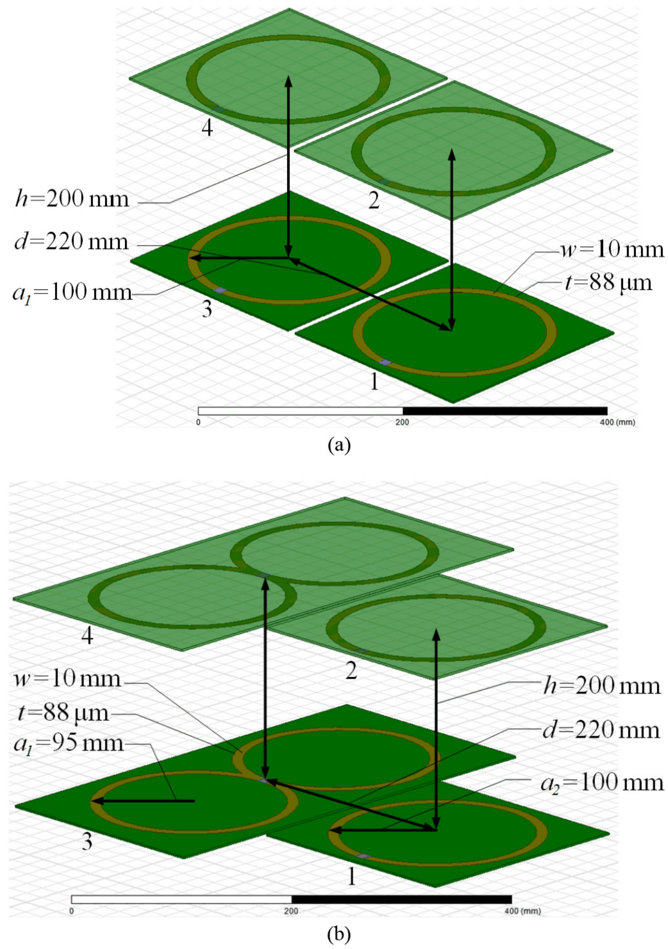

Fig. 4. HFSS simulation model of (a) conventional circular loop antenna array MIMO and (b) heterogeneous multipole loop antenna array MIMO.

The heterogeneous multipole loop antenna array is not limited to a 2×2 MIMO scheme, in which two transmit and two receive antennas are employed. Fig. 6 shows a 3×3 NFMI MIMO example model which consists of a circular loop, a quadrupole loop, and an octupole loop, which has eight magnetic poles. In this case, to satisfy the cancellation conditions, the center of each loop must be placed on the cancellation lines of other antennas. Because the magnetic field strength depends on the radius size, the gain of octupole S65 is smaller than those of other loops. To compensate this smaller gain, we can increase the number of turns or insert ferrite in the center of the octupole loop. Similarly, the heterogeneous antenna array can be implemented for more than three antennas.

C. Verification of Crosstalk Cancellation Via Experiments

We implemented a testbed of 2×2 NFMI MIMO in which the configuration parameters were the same as those in simulations. In these experiments, we tested the crosstalk cancellation

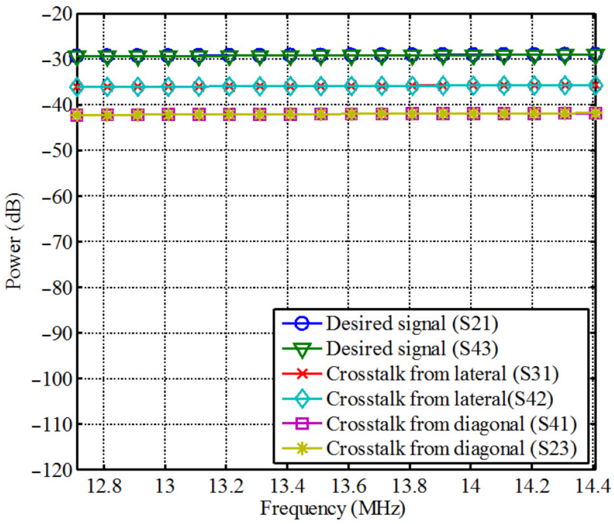

(a)

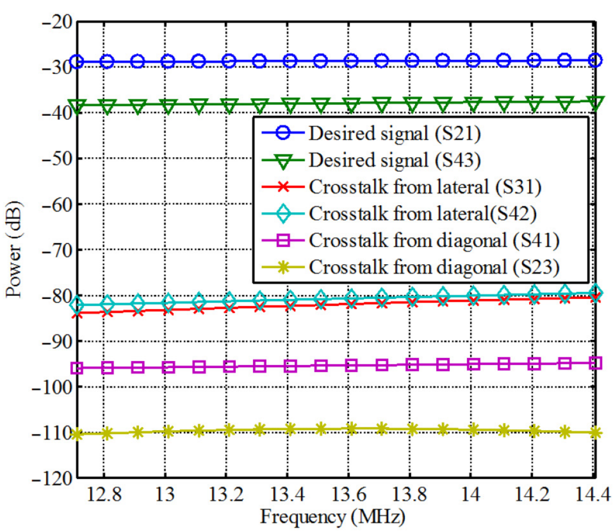

(b)

Fig. 5. Simulation results of (a) conventional circular loop antenna array MIMO and (b) heterogeneous multipole loop antenna array MIMO.

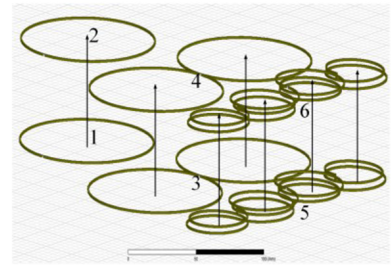

(a)

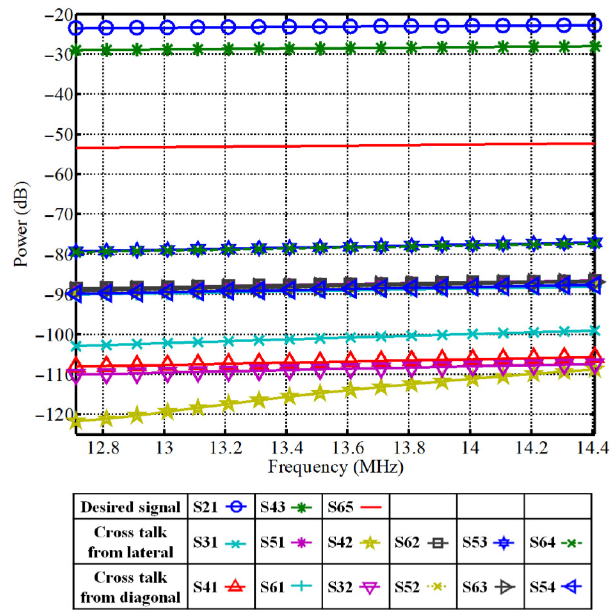

(b)

Fig. 6. (a) Example of NFMI MIMO 3x3 with the heterogeneous multipole loop antenna array for crosstalk cancellation. (b) Gain of the desired and crosstalk signals.

(a)

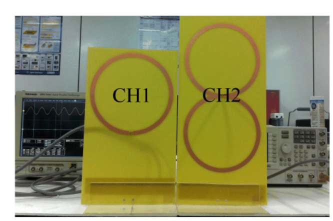

(b)

Fig. 7. Experimental setup using an oscilloscope for crosstalk cancellation. (a) Conventional circular loop antenna array. (b) Heterogeneous multipole loop antenna array.

using two different measurement devices, an oscilloscope and a network analyzer.

To obtain intuitive results, we measured the crosstalk between array components using the oscilloscope as shown in Fig. 7. In each case, we induced a 13.56-MHz sinusoidal wave in the right circular loop CH1. Then, we tested the existence of an induced voltage in the left CH2. When crosstalk occurred, CH2 had induced voltage from the right loop. In the case of the conventional circular loop antenna, crosstalk was very clearly observed in CH2, as shown in Fig. 8(a). On the other hand, in the case of the heterogeneous multipole loop, CH2 did not induce a noticeable signal, as shown in Fig. 8(b), thus verifying the crosstalk cancellation effect.

In the network analyzer experiment, we measured the S-parameter between two ports, and remaining ports are connected with a 50-Ω load as shown in Fig. 9. Note that the crosstalk signal is severer in the conventional antenna pattern, with an SINR of around 0 dB as seen in Fig. 10(a). However, it is reduced significantly for the proposed antenna scheme, with an SINR of around 30 dB for desired signal of the circular loop and around 20 dB for the desired signal of the quadrupole loop, realizing high-quality parallel MIMO channel links. Due to the noise and residual crosstalk with experimental errors such as antenna misalignment, the channel quality became worse compared to the simulation results, with SINR values of 6 and 40 dB for the conventional and proposed antenna patterns, respectively. However, the SINR of 20 dB or more can provide significant channel throughput as seen in the next section.

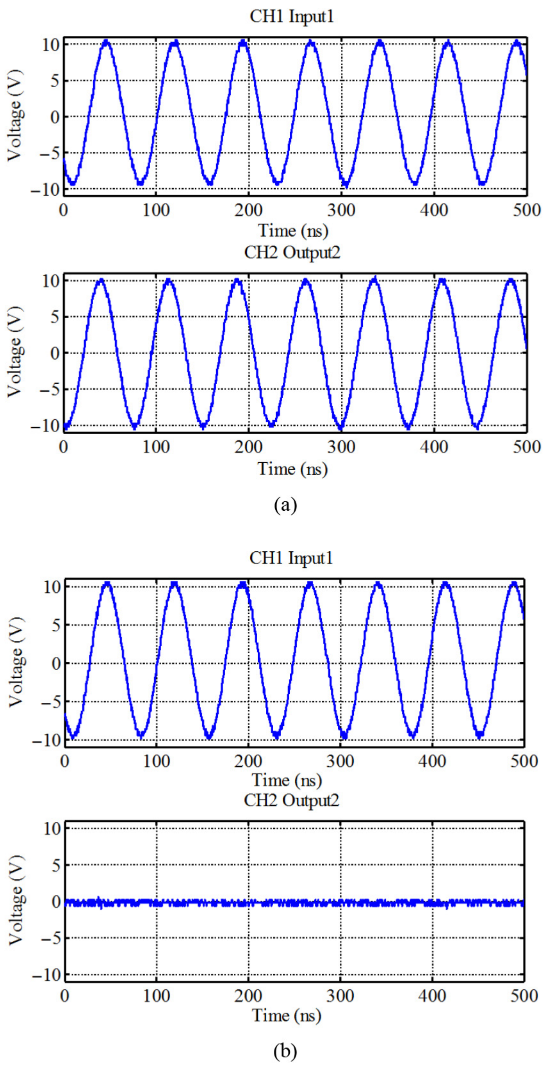

Fig. 8. Experimental results of crosstalk cancellation obtained using oscilloscope (Input: CH1, Output: CH2, $f = 13.56\ MHz$). (a) Conventional circular loop antenna array. (b) Heterogeneous multipole loop antenna array.

Fig. 9. Experimental setup using network analyzer for signal gain measurement of (a) conventional circular loop antenna array MIMO and (b) heterogeneous multipole loop antenna array MIMO.

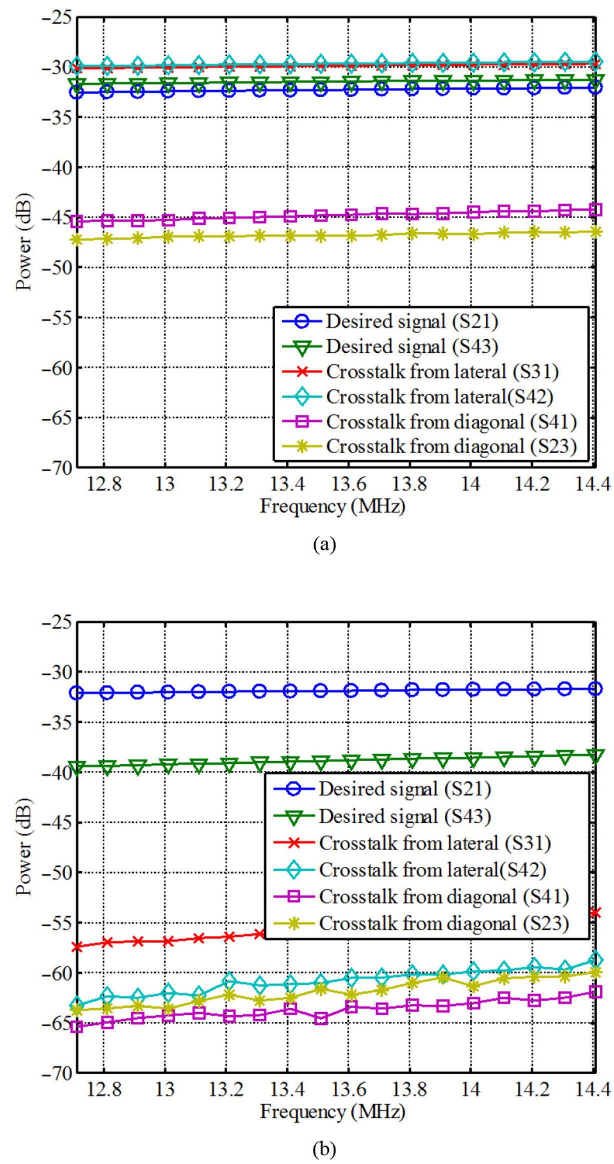

Fig. 10. Experimental results of (a) conventional circular loop antenna array MIMO and (b) heterogeneous multipole loop antenna array MIMO using network analyzer.

III. Capacity Analysis of the Proposed NFMI MIMO

A. Channel Model of NFMI MIMO

In this section, we analyze the performance of the proposed MIMO method and compare it with that of an NFMI single-input single-out (SISO) scheme in terms of channel capacity. We obtain gain and phase information from the S-parameter and group delay in the frequency domain for a channel model using HFSS simulation. The S-parameters of the desired signals represent the real part of channel gain, and group delay represents the channel phase distortion. This gain and phase information can be expressed as a complex channel gain in the frequency domain.

To measure the frequency response of a channel, we need to define the proper channel and bandwidth. We consider the frequency band of an NFC channel having 848-kHz bandwidth at the carrier frequency of 13.56 MHz to see if it is appropriate for MIMO transmission of the proposed scheme. To check whether there is any intersymbol interference (ISI), we measure the delay spread of the channel, the difference of the maximum and minimum delays in the frequency band for comparison with the symbol time duration of $1.1792\ \mu s$ (a reciprocal of the bandwidth of the NFC system). As shown in Fig. 11, the delay

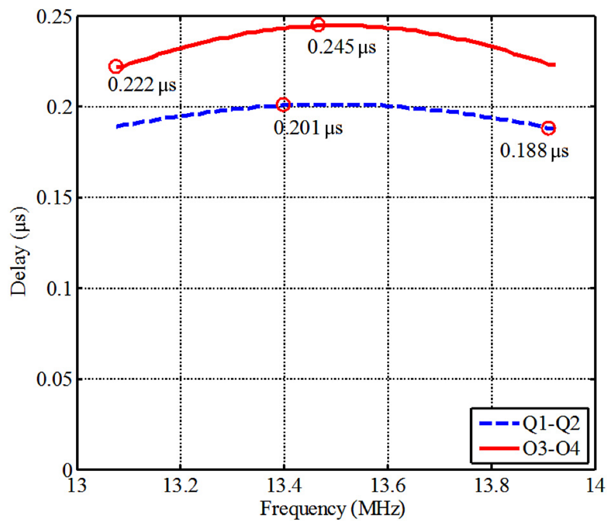

Fig. 11. Delay response of the NFMI MIMO communication system.

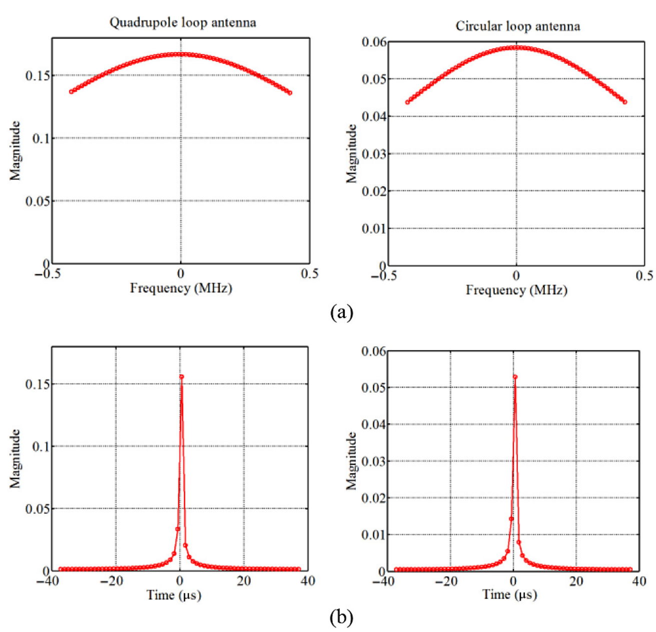

Fig. 12. (a) Frequency and (b) time-domain channel response of the NFMI MIMO channel.

spread of the MIMO channel is $0.057\ \mu s\ (= 0.245 - 0.188)$, corresponding to 4.83% of the symbol time duration. It results in negligible ISI, allowing us to assume that the channel has almost flat response in the frequency domain and equivalently single-path delay in the time domain [20]. For each parallel channel, the frequency and time-domain response of the channel in the desired band are plotted in Fig. 12. The magnitude shows almost flat response as seen in Fig. 12(a). Thus, the time-domain impulse response, which is the inverse Fourier transform of the frequency response, can be regarded as a one-tap finite-impulse response (FIR) filter with negligible delay, as shown in Fig. 12(b), meaning that reflection is not serious, and conventional flat channel MIMO EM channel modeling can be applied in the proposed NFMI MIMO channel as well.

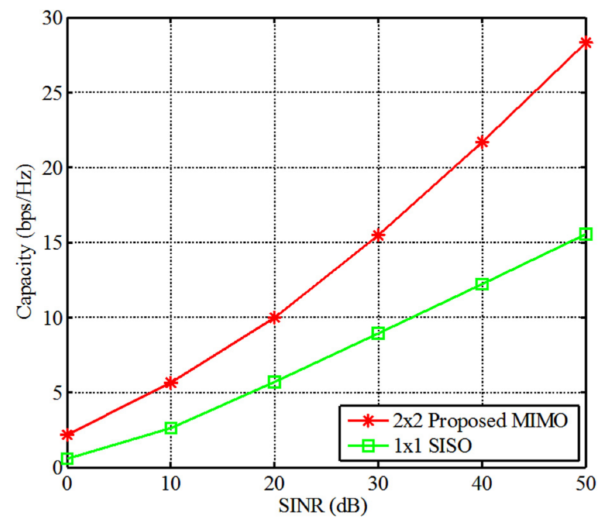

Fig. 13. Channel capacity of SISO and proposed NFMI MIMO system.

B. Channel Capacity of NFMI MIMO

Before the discussion of the proposed method, we need to mention conventional far-field RF MIMO using EM wave. A conventional RF MIMO system can efficiently generate multiple scalar channels using SVD. Therefore, a conventional RF MIMO system can linearly increase the channel capacity, which is upper bound of the data throughput, as much as the number of multiple channels whose number is equal to min (N, M), where N and M are the number of transmit and receive antennas, respectively, [14]. Usually, this advantage is called multiplexing gain. Alternatively, a conventional RF MIMO system can be used to reduce the bit error rate (BER) in fading channels with proper space-time coding. This gain is called diversity gain. The proposed NFMI MIMO scheme can provide multiplexing gain with multiple antennas having zero crosstalk as shown in Section II. It can be realized with low-complexity without complicated channel estimation, which is usually needed in conventional RF MIMO systems for SVD operation, since the proposed scheme can avoid the crosstalk problem by making parallel channels using the simple heterogeneous antenna pattern.

Now, we compute the channel capacity of the proposed NFMI MIMO with N transmit and N receive antennas [14]

$$C_{EP} = \log_2 \left[det \left(I_N + \frac{\rho}{N} H H^* \right) \right] \text{ bps/Hz} \tag{7}$$

where ρ is the SINR of the received signal; I is the identity matrix; H is the $N \times N$ channel matrix; and $*$ is the transpose-conjugate. Fig. 13 plots the channel capacity of a conventional NFMI S ISO system and the proposed NFMI 2×2 MIMO system. We can confirm the gain of the proposed method which has up to two times the capacity of NFMI SISO in high SINR. This result shows almost the same tendency as conventional far-field RF MIMO with SVD and perfect channel information of H. Therefore, the data rate can be enhanced using the proposed NFMI MIMO scheme even for high permittivity channels.

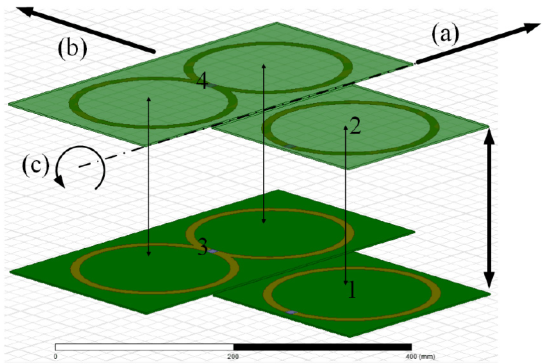

Fig. 14. Misalignment simulation (a) front and rear, (b) left and right, and (c) rotation.

IV. Practical Issue of Misalignment

Generally, the gain of NFMI communication systems is sensitive to the relative positions of a transmitter coil and a receiver coil. The proposed scheme may have a similar misalignment problem since crosstalk cancellation is only available when target antennas are located on the cancellation planes of other antennas. In this section, to investigate the relationship between crosstalk cancellation effect and misalignment, we perform simulation to obtain a link gain without environmental noise for three cases of misalignment in different directions: front and rear [Fig. 15(a)], left and right [Fig. 15(b)], and rotation [Fig. 15(c)] as shown in Fig. 14. Simulations were conducted with the variation in the overlapped area between the transceiver and receiver. When the area of overlap is equal to 100% or the rotation degree is equal to 0°, transceiver and receiver are perfectly aligned with each other. In the cases of horizontal shift, i.e., front and rear [Fig. 15(a)] or left and right [Fig. 15(b)] directions, the gain of the desired signal becomes smaller as the overlap percentage decreases. In the front and rear shifting case, the crosstalk, which is caused by the diagonal movement, increases rapidly, as seen in Fig. 15(a) since the center of the loop deviates from the cancellation plane. In the case of left and right movement, however, the crosstalk does not increase quickly as seen in Fig. 15(b) since the pattern of movement does not deviate much from the cancellation plane, resulting in higher SNR than that of (a). Rotation results in a similar tendency to the case of left and right movement as seen in Fig. 15(c). That is, the effect of the misalignment to the crosstalk cancellation effect differs according to the movement direction and the misalignment errors are less sensitive for the movement in the left and right direction or the rotation. Fig. 16 plots the channel capacity of the proposed MIMO and conventional SISO schemes in the misalignment cases of Fig. 14. Although the capacity degradation increases as the alignment error increases, the MIMO gain over SISO are still large especially for the cases of Fig. 14(b) and (c), implying the benefit with the use of the proposed scheme. Thus, we may employ the proposed scheme in practice particularly for applications where the misalignment error is small or occurs in specific directions, e.g., not in front and rear direction, such as tire pressure sensing and subway position control systems.

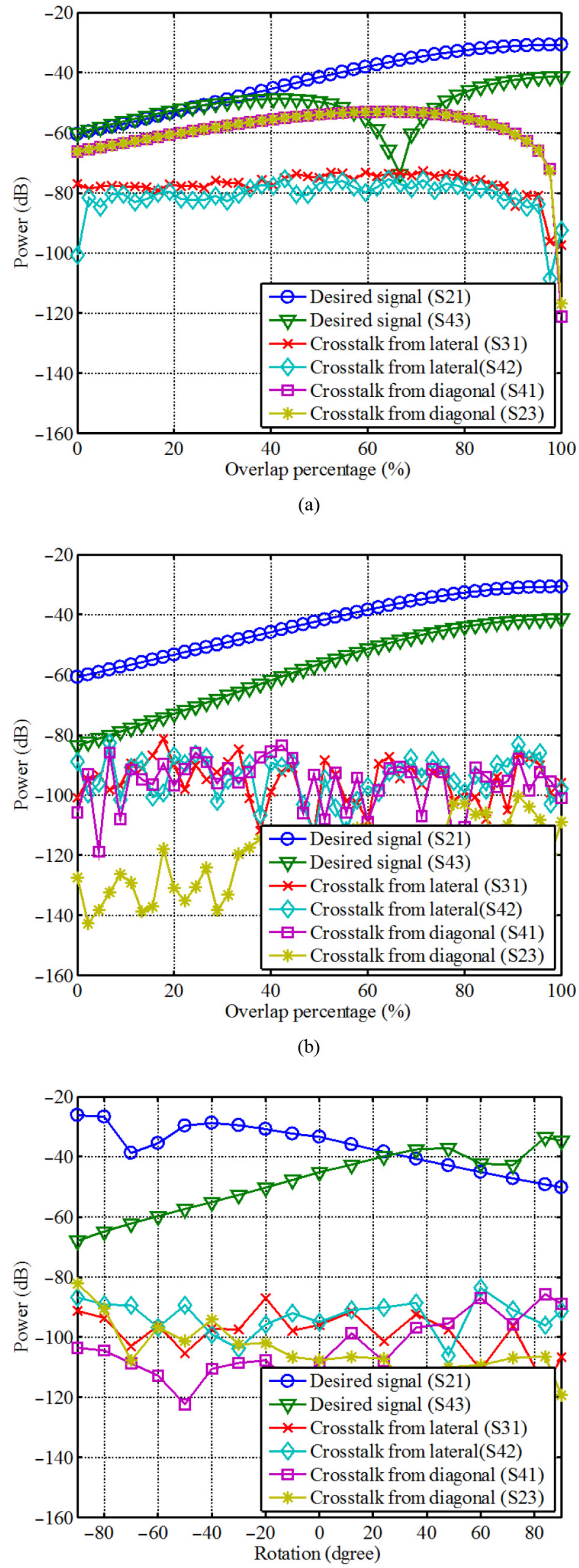

Fig. 15. Gain in the presence of alignment errors in the direction of (a) front and rear, (b) left and right, and (c) rotation.

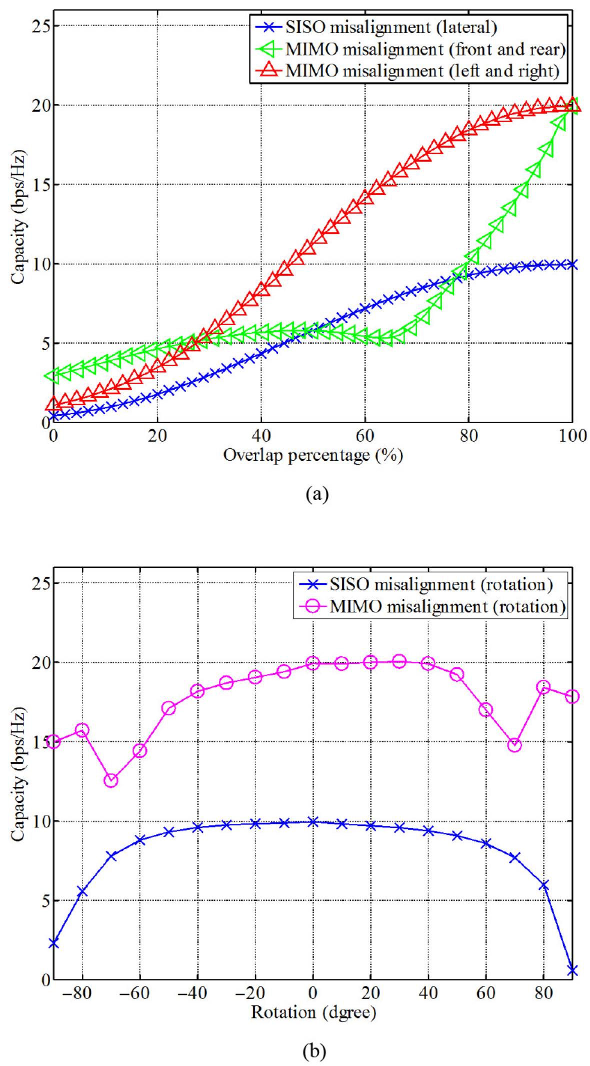

Fig. 16. Channel capacity of misalignment cases (SNR = 30 dB). (a) Planar misalignment. (b) Rotation misalignment.

Besides the misalignment, the cancellation condition may not be satisfied by metallic objects close to an antenna. If the effect of crosstalk is too high to be allowed due to the misalignments of antennas or the presence of arbitrary objects, parallel multi-stream transmission cannot be supported. In this case, we may obtain parallel channels by applying signal processing such as channel estimation and SVD at the cost of computational loads, which will be studied as future work.

V. Conclusion and Potential Applications

In this paper, we proposed an NFMI MIMO communication scheme to increase channel capacity. The proposed heterogeneous multipole antenna array can reduce the crosstalk between transmitters and receivers. As a result, the signals of each pair of antennas can be independently transmitted, realizing MIMO transmission. We verified that crosstalk cancellation is achieved by the proposed method through numerical simulations and experiments. Through channel modeling and capacity calculation, we also confirmed that the enhancement of channel capacity with the proposed NFMI MIMO communication system is similar to that achieved with conventional far-field RF MIMO systems. Furthermore, it does not require complicated processing at the receiver, such as SVD operation and channel estimation, facilitating implementation. The effect of antenna misalignment was also investigated. Large capacity gain can be obtained in the most cases of misalignment and the alignment error needs to be bounded differently according to the direction of misalignment.

The proposed scheme can be applied in various NFC applications requiring high-rate transmission, such as smart poster and cellular device data sharing. It could be also applied in high permittivity channel environments, such as underwater, underground, and in-body applications. As an example of in-body medical implant communications, our proposed scheme can increase the temporal resolution and number of channels for wireless cochlear implants, enabling enhancement of perceived sound quality. Furthermore, our proposed scheme can be applied to intraocular retinal prosthesis for a larger number of electrodes and higher resolution [4]. In addition, our proposed scheme can simultaneously transmit data and power to various devices, allowing an integrated magnetic system which would enable communication and wireless power transmission at the same time.

References

[1] S. Kisseleff, I. F. Akyildiz, and W. H. Gerstacker, "Throughput of the magnetic induction based wireless underground sensor networks: Key optimization techniques," *IEEE Trans. Commun.*, vol. 62, no. 12, pp. 4426–4439, Dec. 2014.

[2] M. C. Domingo, "Magnetic induction for underwater wireless communication networks," *IEEE Trans. Antennas Propag.*, vol. 60, no. 6, pp. 2929–2939, Jun. 2012.

[3] V. K. K. K. Pasumarthi and A. V. Paramkusam, "An intelligent defense security system for armory," *Int. J. Prof. Eng. Stud.*, vol. 4, no. 2, pp. 43–47, Oct. 2014.

[4] A. Yakovlev, S. Kim, and A. S. Y. Poon, "Implantable biomedical devices: Wireless powering and communication," *IEEE Commun. Mag.*, vol. 50, no. 4, pp. 152–159, Apr. 2012.

[5] Z. Sun and I. F. Akyildiz, "Underground wireless communication using magnetic induction," in *Proc. IEEE Int. Conf. Commun. (ICC'09)*, Jun. 2009, pp. 1–5.

[6] Z. Sun, I. F. Akyildiz, S. Kisseleff, and W. Gerstacker, "Increasing the capacity of magnetic induction communications in RF-challenged environments," *IEEE Trans. Commun.*, vol. 61. no. 9, pp. 3943–3952, Sep. 2013.

[7] V. Coskun, O. Busra, and O. Kerem, "A survey on near field communication (NFC) technology," *Wireless Pers. Commun.*, vol. 71, no. 3, pp. 2259–2294, Aug. 2013.

[8] M. Patel and J. Wang, "Applications, challenges, and prospective in emerging body area networking technologies," *IEEE Trans. Wireless Commun.*, vol. 17, no. 1, pp. 80–88, Feb. 2010.

[9] A. S. Poon, S. O'Rdiscoll, and T. H. Meng, "Optimal frequency for wireless power transmission into dispersive tissue," *IEEE Trans. Antennas Propag.*, vol. 58, no. 5, pp. 1739–1750, May 2010.

[10] E. Shamonina, V. A. Kalinin, K. H. Ringhofer, and L. Solymar, "Magneto-inductive waveguide," *IET Electron. Lett.*, vol. 38, no. 8, pp. 371–373, Apr. 2002.

[11] M. Masihpour, D. Franklin, and M. Abolhasan, "Multihop relay techniques for communication range extension in near-field magnetic induction communication systems," *J. Netw.*, vol. 8, no. 5, pp. 999–1011, May 2013.

[12] H. Nguyen, J. I. Agbinya, and J. Devlin, "Channel characterisation and link budget of MIMO configuration in near field magnetic communication," *Int. J. Electron. Telecommun.*, vol. 59, no. 3, pp. 255–262, Aug. 2013.

[13] R. B. Gottula, "Discrete-time implementation, antenna design, and MIMO for near-field magnetic induction communications," Ph.D. dissertation, Dept. ECE, Univ. Brigham Young, Provo, UT, USA, 2012.

[14] D. Gesbert, M. Shafi, D. S. Shiu, P. Smith, and A. Naguib, "From theory to practice: An overview of MIMO space-time coded wireless systems," *IEEE J. Sel. Areas Commun.*, vol. 21, no. 3, pp. 281–302, Apr. 2003.

[15] K. Finkenzeller, *RFID Handbook: Radio-Frequency Identification Fundamentals and Applications*, 3rd ed. Hoboken, NJ, USA: Wiley, 2004, pp. 61–110.

[16] Z. D. Deng, S. H. Lisanby, and A. V. Peterchev, "Coil design considerations for deep transcranial magnetic stimulation," *Clin. Neurophysiol.*, vol. 125, no. 6, pp. 1202–1212, Jun. 2014.

[17] S. J. Koerner, "Inductive loop structure for detecting the presence of vehicles over a roadway," U.S. Patent 3 984 764, Mar. 3, 1976.

[18] B. Johannisson, A. Derneryd, and M. Johansson, "Dual-polarized antenna," U.S. Patent 6 531 984, Oct. 27, 2003.

[19] Ansoft Corporations, *ANSYS HFSS V.14*, Pittsburgh, PA, 2014.

[20] Y. S. Cho, J. Kim, W. Y. Yang, and C. G. Kang, *MIMO-OFDM Wireless Communications With MATLAB*. Hoboken, NJ, USA: Wiley, 2010, pp. 16–19.

Han-Joon Kim (S'15) received the B.S. and M.S. degrees in information control and instrumentation engineering from Kwangwoon University, Seoul, South Korea, in 2011 and 2013, respectively. He is currently pursuing the Ph.D. degree in information and communication engineering at Daegu Gyeongbuk Institute of Science and Technology (DGIST), Daegu, South Korea.

His research interests include magnetic communication, wireless power transfer, and transcranial magnetic stimulation.

Jinho Park (S'99–M'03) received the B.S. degree in electrical engineering from Seoul National University, Seoul, South Korea, in 1996, and the Ph.D. degree in electrical engineering from the University of Washington, Seattle, WA, USA, in 2003.

He worked with Marvell Semiconductor, Santa Clara, CA, USA, from 2003 to 2012, leading the analog and RF design aspects of the world's first 802.11ac mobile MIMO IC publicly announced in June, 2012. He is currently with TeraSquare Co. Ltd., Seoul, South Korea, fabless 100 Gbps ethernet IC Company, as a CEO and an Adjunct Professor with the Department of Information and Communication Engineering, Daegu Gyeongbuk Institute of Science and Technology (DGIST), Daegu, South Korea. He is the coauthor of *Parasitic-Aware Optimization of CMOS RF Circuits* (Kluwer Academic) in 2003 and has more than 60 IEEE publications and U.S. patents.

Kyoung-Sub Oh received the B.S. degree in electrical engineering from Chonbuk National University, Jeonju, South Korea, in 1994, and the M.S. and Ph.D. degrees in electrical engineering from the Korea Advanced Institute of Science and Technology (KAIST), Daejeon, South Korea, in 1997 and 2004, respectively.

From 2004 to 2005, he worked with Hyundai Motor, Gyeonggi-do, Hwaseong-si, Korea. He also served Maltani Lighting, Seoul, Korea, Samung Electronics, Gyeonggi-do, Hwaseong-si, Korea, and KAIST from 2005 to 2008, from 2008 to 2010, and from 2010 to 2014, respectively. Since 2014, he has been a Principal Research Engineer with Gamma Nu, Hwasung, South Korea. His research interests include base station antenna, in-building antenna, microwave imaging, inverse scattering, wireless power transfer, and wireless communication system.

Jihwan P. Choi (S'00–M'06) received the B.S. degree in electrical engineering from Seoul National University, Seoul, South Korea, in 1998, and the S.M. and Ph.D. degrees in electrical engineering and computer science from Massachusetts Institute of Technology (MIT), Cambridge, MA, USA, in 2000 and 2006, respectively.

From 2006 to 2012, he was a Principal System Engineer with the Wireless Research and Development Group, Marvell Semiconductor, Santa Clara, CA, USA, for mobile system design and standardization of third- and fourth-generation commercial wireless communications, including worldwide interoperability for microwave access (WiMAX) and the third-generation partnership project long-term evolution (LTE). He is currently an Assistant Professor with the Department of Information and Communication Engineering, Daegu Gyeongbuk Institute of Science and Technology, Daegu, South Korea. His research interests include cross-layer system design for space and wireless networks, and wireless power transfer technologies.

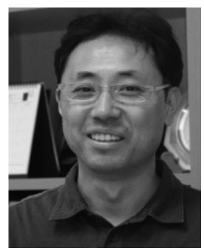

Jae Eun Jang received the B.S. and M.S. degrees in material engineering from Hanyang University, Seoul, South Korea, in 1994 and 1996, respectively, and the Ph.D. degree in electrical engineering from the University of Cambridge, Cambridge, U.K., in 2006.

From 2007 to 2011, he was a Principal Senior Researcher with the Samsung Advanced Institute of Technology, Yongin, South Korea. Since 2011, he has been a Professor of Information and Communication Engineering with the Daegu Gyeongbuk Institute of Science and Technology (DGIST), Daegu, South Korea. He first demonstrated mechanical nanoswitch and mechanical DRAM concept using vertically aligned carbon nanotube in 2004 and 2008, respectively. He has authored or coauthored more than 80 journal and conference papers and is an inventor of 80 granted patents. His research interests include nanodevices for communication area and biomimic sensor.

Ji-Woong Choi (S'00–M'04–SM'09) received the B.S., M.S., and Ph.D. degrees from Seoul National University (SNU), Seoul, South Korea, in 1998, 2000, and 2004, respectively, all in electrical engineering.

From 2004 to 2005, he worked as a Postdoctoral Researcher with the Inter-University Semiconductor Research Center, SNU. From 2005 to 2007, he was a Postdoctoral Visiting Scholar at the Department of Electrical Engineering, Stanford University, Stanford, CA, USA. He also worked as a Consultant with GCT Semiconductor, San Jose, CA, USA, for the development of mobile TV receivers from 2006 to 2007. From 2007 to October 2010, he worked with Marvell Semiconductor, Santa Clara, CA, USA, as a Staff Systems Engineer for next-generation wireless communication systems, including WiMAX and LTE. Since October 2010, he has been with the Department of Information and Communication Engineering, Daegu Gyeongbuk Institute of Science and Technology (DGIST), Daegu, South Korea, as an Associate Professor. His research interests include wireless communication theory, signal processing, biomedical communication applications, and brain–machine interface.